Leuven, Belgium, May 1998

Pipelined Sampling Techniques for Sonar Tracking Systems

Uwe D. Hanebeck
Institute of Automatic Control Engineering (LSR)
Technische Universität München
80290 München, GERMANY
e-mail: Uwe.Hanebeck@e-technik.tu-muenchen.de

Abstract

This paper introduces fast sampling strategies for pulse–echo time–of–flight sonar using time multiplexing. As a result, multiple interlaced measurement streams are employed to achieve high sampling rates without sacrificing range accuracy. The method considers receiver blanking constraints caused by imperfect acoustic decoupling between transmitter and receivers. Furthermore, uncertainties due to measurement noise and moving targets are taken into account. The proposed approach has been experimentally validated for sampling rates of up to 450 Hz with a multi sonar system mounted on a mobile robot.

1 Introduction

This paper is concerned with fast sampling techniques for pulse–echo time–of–flight sonar sensors. The presented techniques are aimed at mobile robot applications with sonar sensors operating in air. Sonar sensors possess some unique features making them especially well suited for mobile robot applications. Their small size allows direct mounting onto the robot's hull. Thanks to active sensing, measurement results are satisfactory for a wide range of environmental conditions. Furthermore, sonar sensors provide direct geometric information, are inexpensive, and maintenance–free.

Sonar sensors are commonly rated as being inaccurate and unreliable while supplying data at a low rate. However, many researchers have proven sonar to be a reliable sensor for mobile robot applications [1, 2, 3, 4, 5] when using appropriate sensor models and data fusion techniques. Recent research results suggest sensor arrays rather than independent sensors to obtain more than pure distance information [6]. The two–dimensional case (one transmitter and two or three receivers) is treated in [7, 8, 9, 10]. High–precision localization based on two transmitters and two receivers has been reported in [11]. An extension to three dimensions is given in [12].

Erroneous samples caused by cross–talk between sensors may be detected according to the technique presented in [13]. Methods for eliminating cross–talk problems by means of coded excitation are reported in [14, 15]. The latter one is a very promising tool for designing next–generation sonar systems based on low bandwidth transducers.

In this paper, a fast sonar sampling technique is introduced, that remedies the problem of low data rates in single target tracking applications, which for example occur in the context of mobile robot localization.

The paper is organized as follows: A problem formulation is given in Sec. 2. Standard measurement techniques are reviewed in Sec. 3.1, the new pipelined sampling scheme is introduced in Sec. 3.2. Section 3.3 then proposes a simplified pipelined sampling technique, ambiguity resolution is discussed in Sec. 3.4. Experimental results are presented in Sec. 4 and followed by concluding remarks given in Sec. 5.

2 Problem Formulation

We consider a three–dimensional arrangement of a sonar transmitter and N receivers, which are placed at known, but arbitrary positions.

The position of a single target is determined by transmitting short ultrasonic bursts and measuring the travel times T_i, $i = 1, \ldots, N$, from the transmitter to the receivers via the target. With the known velocity of sound in air c, associated distances R_i are calculated according to $R_i = cT_i$, Fig. 1. Based on these distances R_i, the position of planar or point–like targets can be calculated for example with the closed–form solutions proposed in [16].

Due to the small velocity of sound in air, this kind of pulse–echo ranging device usually provides data at a rather low rate. Furthermore, measurements may be corrupted by multi–path reflections or environmental noise. This paper introduces a measurement technique, which on one hand increases the sampling rate by employing several measurement streams in parallel. On the other hand, receiver windowing is used to

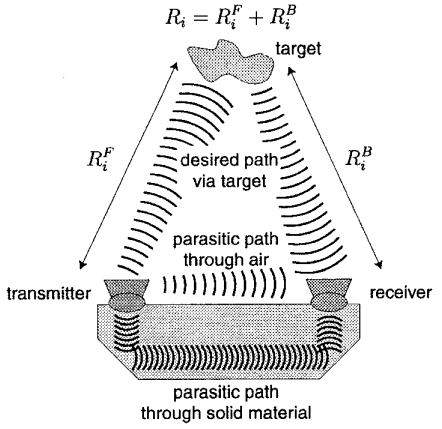

Figure 1: Desired and parasitic signal paths for a pulse–echo ranging system.

simultaneously reduce the probability of false measurements.

In addition, parasitic signal paths from the transmitter to the receivers must be considered in most real–world ranging systems. These parasitic paths are caused by imperfect acoustical decoupling, Fig. 1. One of them is made up by solid material, allows for fast travel of sound waves, and provides little attenuation. The second path is given by the direct connection through air.

While receiving the parasitic signals, the receivers are "blind" for the much weaker target echoes. Hence, the affected receivers are shut off during the associated time period, which is called receiver blanking [17]. The method to be proposed in Sec. 3 will consider this effect in such a way that target echoes are not truncated by receiver blanking.

3 Sampling Methods

In the following, standard sampling with ultrasonic time–of–flight sensors is reviewed. Subsequently, pipelined sampling methods are introduced. For simplicity, only one transmitter / receiver pair is considered in all cases.

3.1 Standard Sampling

The standard operation of an ultrasonic transmitter/receiver pair for range measurements in pulse–echo mode is as follows: With pulse transmission, the receiver is deactivated because of fast parasitic signals through solid material. Reactivation is then performed after the time interval T^{blank}, when the slower parasitic signals through air have also died out. The receiver then stays activated for the travel time of the burst from transmitter to receiver via the farthest considered target. Before transmitting the next pulse, an additional waiting interval is often inserted to allow multi–path reflections to die out.

In case of a single target, the next pulse may immediately be transmitted after the echo return. Hence, the sampling rate increases with decreasing target distance. Nevertheless, large portions of the available channel capacity remain unused. Exploiting the fact, that the k–th target echo return time T_k^P can be predicted on the basis of previous measurements, it is sufficient to activate the receiver in a window of width $2T_k^F$ centered around T_k^P, Fig. 2 a). The window width $2T_k^F$ is a function of the relative velocity between target and measurement device and the measurement uncertainty. The resulting unused time intervals can be filled with additional measurement sequences.

3.2 Pipelined Sampling

In this section, the general concept of pipelined or time–multiplexed sampling is introduced. In Sec. 3.3, a simplified version will be presented, which may be used with off–the–shelf sensors.

The basic idea of pipelined sampling is to use more than one measurement stream at a time. Several measurement streams are interlaced in such a way, that additional pulses are already transmitted, when a measurement sequence is still in progress, Fig. 2 b), c). Hence, a measurement pipeline is set up. Of course, the measurement time for a specific pulse remains unchanged. Nevertheless, a larger number of pulses per unit time are obtained.

When N interlaced measurement sequences are employed in parallel, the unused time interval between transmitting and receiving for a single measurement sequence must be wide enough to hold another $N-1$ sequences, i.e,

$$T^P \geq N\,T^{\text{blank}} + (2N-1)\,T^F \quad . \tag{1}$$

The sampling rate is given by

$$R_s = \frac{N}{T^P + T^F} \quad . \tag{2}$$

Figure 3 shows the sampling rate as a function of the target distance for different N. The bold line characterizes the case when the maximum number of parallel measurement sequences $N_{\max}$ is employed.

The required prediction T^P of the echo return time can be derived from two different sources: 1. On the basis of previous measurements. In this case, a tracking control loop tries to center the echoes within the receive windows. 2. Based on a priori information about the target location. This is for example the case in mobile robot localization, where the prediction can

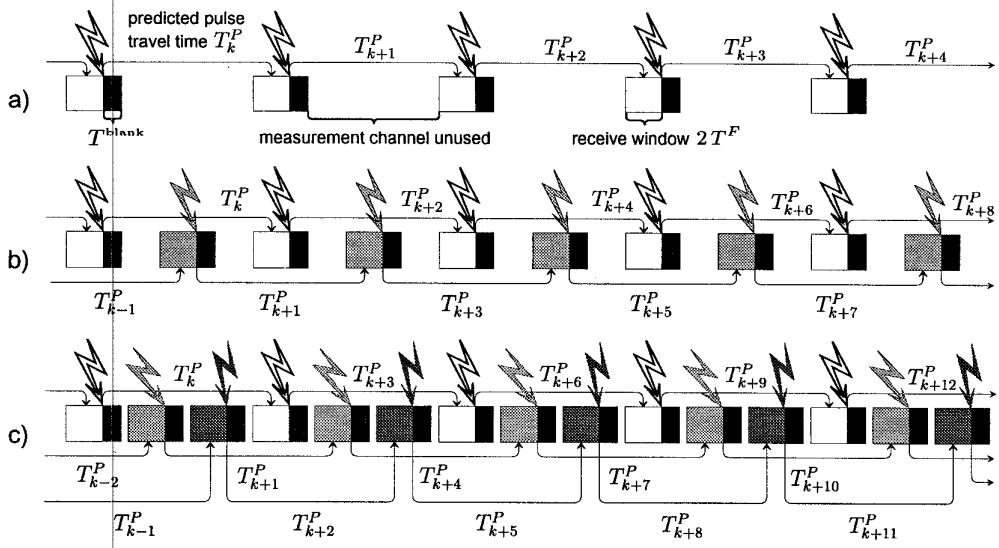

Figure 2: a) Fastest sequential measurement sequence with receiver activation window of width $2T_k^F$. b) Two, c) Three interlaced measurement sequences. □, ▒, ■ denote sequence 1, 2, and 3, respectively. ⇝ denotes pulse transmission. ■ denotes the blanking period.

be performed on the basis of the robot location and a given landmark map.

The proposed sampling scheme makes maximum use of the available channel capacity while meeting all constraints, i.e., receiver blanking and measurement uncertainties are considered so that the target echoes are received without truncation. Hence, accuracy is not reduced. In addition, the large number of samples allows the application of advanced filtering techniques for the purpose of noise reduction.

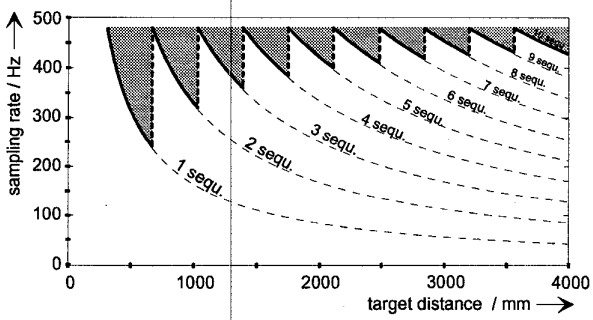

Figure 3: Theoretical sampling rate for a transmitter / receiver pair in air using pipelined sampling given a temperature of 293 K, a receiver blanking time of $T^{\text{blank}} = 1.5$ msec, and a fixed receive window width of $2T_k^F = 0.6$ msec.

3.3 Simplified Pipelined Sampling

Many off–the–shelf sonar sensors employ hardwired sampling mechanisms. In most cases, receiver blanking starts with pulse transmission and is immediately succeeded by receiver activation. To perform fast sampling with this kind of sensors, a simplification is introduced. For that purpose, the measurement sequences in Fig. 2 are rearranged, so that the receive windows immediately begin after the blanking periods.

A Nassi–Shneiderman diagram of the simplified fast sampling technique is given in Fig. 5, the associated time chart is shown in Fig. 4. The sampling rate achieved

$$R_s = \frac{N-1}{T^P - T^{\text{blank}} - T^F} \tag{3}$$

is a little less compared to the optimal sampling rate in Fig. 3.

3.4 Ambiguity Resolution

Performing pipelined sampling according to the methods presented in the last two sections yields ambiguous range measurements. For a single target, ambiguity was resolved by using the predicted echo return time T_k^P for the considered target, which is updated with every new sample.

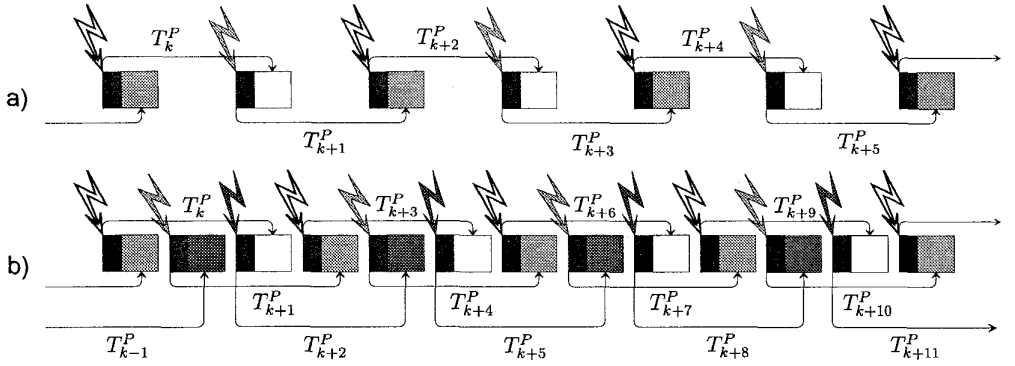

Figure 4: Simplified uniform pipelined sampling. a) Two, b) Three parallel measurement sequences.

When additional targets are present, two cases occur. In the first case, additional echoes fall into the unused time intervals between receiver activation intervals. Hence, appropriate receiver windowing as introduced in Sec. 3.3 and Sec. 3.2 is sufficient for avoiding ambiguity. In the second case, additional echoes fall into the receiver activation windows for the main target. This requires extra considerations for ambiguity resolution.

For that purpose, the transmission times (with respect to the previous transmission) are modulated by a triangular modulation sequence, Fig. 6 a). As a result,

Select the number of interlaced measurement sequences. The maximum number is given by rearranging (1) as $N_{\max} = \text{Floor}\left(\frac{T^P+T^F}{T^{\text{blank}}+2T^F}\right)$
Wait for $\frac{T^P-T^{\text{blank}}-T^F}{N-1}$
Transmit pulse; $\ldots$, $t_2 = t_1$, $t_1 = t_0$, t_0=now
Wait for T^{blank}
Activate receiver
Wait until $t_0 + T^{\text{blank}} + 2T^F$, t_{echo} $\ldots$ echo return time
Deactivate receiver
Range $R = c\,\{[t_0 - t_{N-1}] + [t_{\text{echo}} - t_0]\}$

Figure 5: Simplified pipelined sampling.

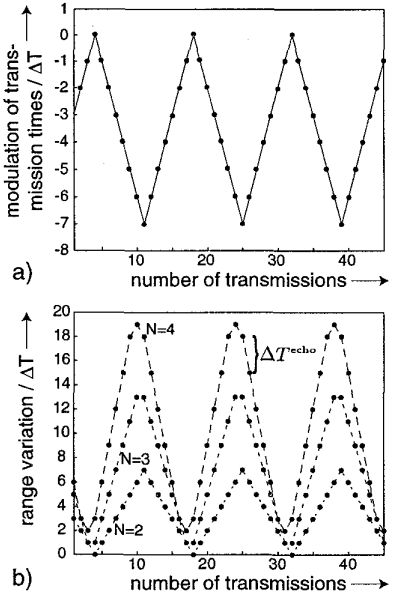

Figure 6: Modulation of relative transmission times. a) Modulation sequence. b) Resulting sequence of range variations for two, three, and four interlaced measurement sequences.

the sampling frequency is periodically varied. The resulting sequence of ranges measured with respect to the last transmission is shown in Fig. 6 b) for two, three, and four interlaced measurement sequences. It is obvious, that the range ambiguity can be resolved on the basis of the range changes over time according to

$$N = \frac{\Delta T^{\text{echo}}}{\Delta T} + 1 \ . \qquad (4)$$

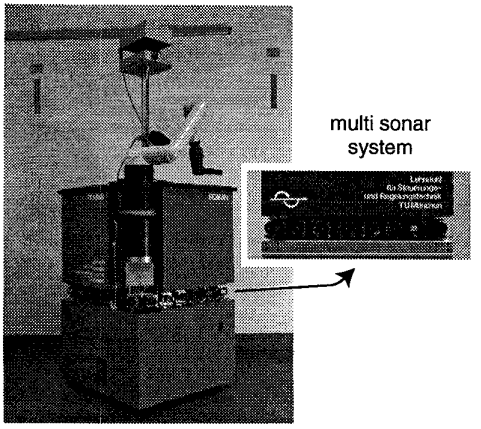

Figure 7: Mobile service robot ROMAN equipped with multi sonar system.

ΔT should be chosen large enough to have a sufficiently large effect in the presence of noise. On the other hand, the triangular modulation sequence must be long enough to validate the largest considered N. Nevertheless, the constraint (1) must be kept all the time to prevent truncation of desired target echoes.

The conclusion of this section is, that it is not always appropriate to work with the maximum number $N_{\max}$ of interlaced measurement streams, because outlier elimination based on sampling rate variations can only be performed if there are unused time intervals available. Hence, in practical applications, $N < N_{\max}$ is used to cope with outliers.

4 Experimental Validation

For experimental validation of the proposed sampling techniques, the mobile service robot ROMAN is used, Fig. 7, which is equipped with a multi sonar sensor system [18]. A simple experiment is conducted, where ROMAN measures the relative location of a wall while driving back and forth at a velocity of 200 mm/sec.

For measurement purposes, ROMAN employs a single ultrasonic transmitter and an array of 5 receivers oriented towards the wall under consideration. Furthermore, the robot's internal sensors are used. Similar to the work presented in [19], fusion of the ultrasonic sensors and the internal sensors is performed in a set–theoretic framework. Given the current uncertainty of the relative wall location and the relative velocity, a receive window T_k^F is calculated for the next measurement.

The results are shown in Fig. 8 and Fig. 9. Fig. 8 a) shows the **raw** distances as being measured between the transmitter, the wall, and one of the receivers. The sampling rate achieved is shown as a function of time

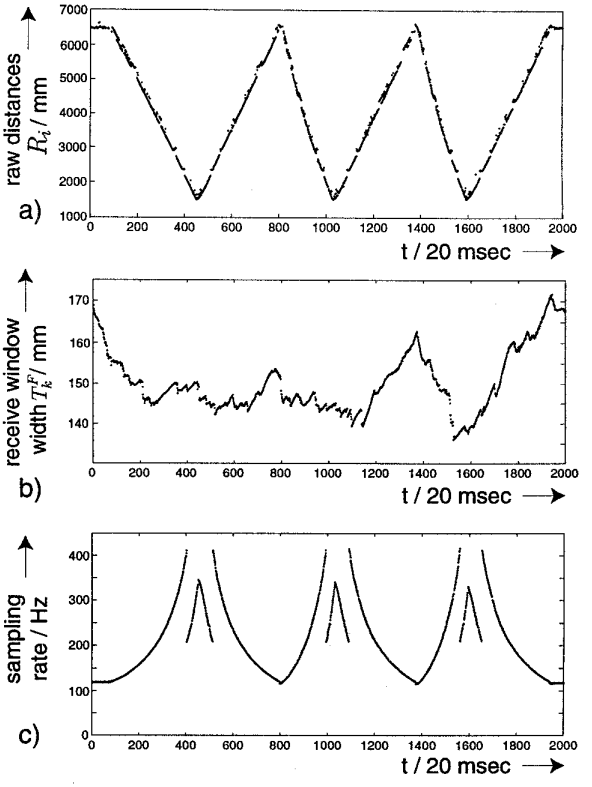

Figure 8: Experimental results. a) Measured range. b) receive window width T^F. c) Sampling rate.

in Fig. 8 c). The associated receive window width T_k^F is given in Fig. 8 b).

Fig. 9 shows the sampling rate as a function of the measured distance. The result is in good accordance with the theoretical results given for a fixed receive window width in Sec. 3.3. The vertical extent is caused by the time–varying receive window width T_k^F shown in Fig. 8 b).

Commercial threshold detectors are used for measuring echo arrival times. The threshold is time–varying and tuned to standard sampling by the manufacturer, i.e., decreases with time after receiver activation to account for echo attenuation. Hence, the threshold is not appropriate for pipelined sampling, since even echoes from distant targets are obtained shortly after receiver activation. As a result, measurement noise grows with the number of interlaced measurement sequences, which is therefore limited to three in the experiment. To summarize, this effect is not caused by the principle of pipelined sampling and will be eliminated by employing more sophisticated echo detectors.

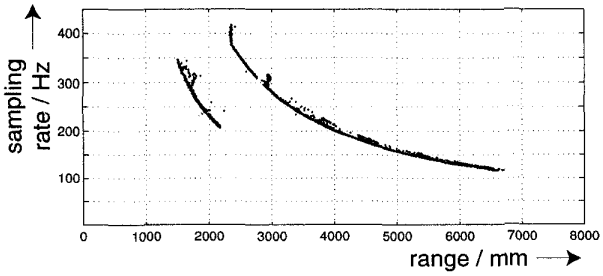

Figure 9: Sampling rate as a function of the distance transmitter → target → receiver.

5 Conclusions

A fast sampling technique for pulse–echo time–of–flight sonar has been proposed and experimentally validated. Besides the general method that makes optimal use of the available channel capacity, also a simplified method is introduced, which may be applied with off–the–shelf sensors.

The presentation was limited to the single transmitter, single target case, which is especially useful for mobile robot localization with respect to a sparse landmark configuration. However, the results given can easily be extended to several transmitters and multiple targets. Furthermore, the proposed method could be combined with the results in [14, 15] in the case of several transmitters.

References

[1] Y. Ando, T. Tsubouchi, and S. Yuta, "A Reactive Wall Following Algorithm and Its Behavior of an Autonomous Mobile Robot with Sonar Ring," *Journal of Robotics and Mechatronics*, vol. 8, no. 1, pp. 33–39, 1996.

[2] J. L. Crowley, "World Modeling and Position Estimation for a Mobile Robot Using Ultrasonic Sensing," in *Proc. of the 1989 IEEE Int. Conf. on Robotics and Automation, Scottsdale, Arizona*, pp. 674–680, 1989.

[3] A. Curran and K. J. Kyriakopoulos, "Sensor-Based Self–Localization for Wheeled Mobile Robots," in *Proc. of the 1993 IEEE Int. Conf. on Robotics and Automation, Atlanta, Georgia*, pp. 8–13, 1993.

[4] A. Curran and K. J. Kyriakopoulos, "Ultrasonic Navigation for a Wheeled Nonholonomic Vehicle," *Journal of Intelligent and Robotic Systems*, vol. 12, no. 3, pp. 239–258, 1995.

[5] J. Leonard and H. F. Durrant-Whyte, "Mobile Robot Localization by Tracking Geometric Beacons," *IEEE Trans. on Robotics and Automation*, vol. 7, no. 3, pp. 376–382, 1991.

[6] Y. Nagashima and S. Yuta, "Ultrasonic Sensing for a Mobile Robot to Recognize an Environment – Measuring the Normal Direction of Walls –," in *Proc. of the 1992 IEEE/RSJ Int. Conf. on Intelligent Robots and Systems, Raleigh, NC*, pp. 805–812, 1992.

[7] L. Kleeman, "A Three Dimensional Localiser for Autonomous Robot Vehicles," *Robotica*, vol. 13, pp. 87–94, 1995.

[8] R. Kuc and B. Barshan, "Bat–Like Sonar for Guiding Mobile Robots," *IEEE Control Systems Magazine*, vol. 12, no. 4, pp. 4–12, 1992.

[9] H. Peremans, K. Audenaert, and J. Van Campenhout, "A High–Resolution Sensor Based on Tri–Aural Perception," *IEEE Trans. on Robotics and Automation*, vol. 9, no. 1, pp. 36–48, 1993.

[10] A. M. Sabatini and O. D. Benedetto, "Towards a Robust Methodology for Mobile Robot Localisation Using Sonar," in *Proc. of the 1994 IEEE Int. Conf. on Robotics and Automation, San Diego, California*, pp. 3142–3147, Mai 1994.

[11] L. Kleeman and R. Kuc, "Mobile Robot Sonar for Target Localization and Classification," *The International Journal of Robotics Research*, vol. 14, no. 4, pp. 295–318, 1995.

[12] H. Akbarally and L. Kleeman, "A Sonar Sensor for Accurate 3D Target Localisation and Classification," in *Proc. of the 1995 IEEE Int. Conf. on Robotics and Automation, Nagoya, Japan*, pp. 3003–3008, 1995.

[13] J. Borenstein and Y. Koren, "Error Eliminating Rapid Ultrasonic Firing for Mobile Robot Obstacle Avoidance," *IEEE Trans. on Robotics and Automation*, vol. 11, no. 1, pp. 132–138, 1995.

[14] K.-W. Joerg and M. Berg, "First Results in Eliminating Crosstalk & Noise by Applying Pseudo-Random Sequences to Mobile Robot Sonar Sensing," in *Proc. of the 1996 IEEE/RSJ International Conference on Intelligent Robots and Systems, Osaka, Japan*, pp. 292–297, 1996.

[15] A. M. Sabatini and A. Rocchi, "Digital–Signal–Processing Techniques for the Design of Coded Excitation Sonar Ranging Systems," in *Proc. of the 1996 IEEE Int. Conf. on Robotics and Automation, Minneapolis, Minnesota*, pp. 335–340, 1996.

[16] U. D. Hanebeck and G. Schmidt, "Closed–Form Elliptic Location with an Arbitrary Array Topology," in *Proc. of the 1996 IEEE Int. Conf. on Acoustics, Speech, and Signal Processing, Atlanta, Georgia*, vol. 6, pp. 3070–3073, 1996.

[17] M. I. Skolnik, *Introduction to Radar Systems*. McGraw–Hill, 1981.

[18] U. D. Hanebeck and G. Schmidt, "A New High Performance Multisonar System for Fast Mobile Robot Applications," in *Intelligent Robots and Systems 1994 (IROS'94)* (V. Gräfe, ed.), pp. 1–14, Amsterdam: Elsevier Science, 1995.

[19] U. D. Hanebeck and G. Schmidt, "Set–theoretic Localization of Fast Mobile Robots Using an Angle Measurement Technique," in *Proc. of the 1996 IEEE Int. Conf. on Robotics and Automation, Minneapolis, Minnesota*, vol. 2, pp. 1387–1394, 1996.